Published in final edited form as:
Circ Arrhythm Electrophysiol. 2010 October ; 3: 624–631. doi:10.1161/CIRCEP.110.945295.

Determinants of Post-Infarction Ventricular Tachycardia

Thomas Crawford, MD, **Jennifer Cowger, MD, MS**, **Benoit Desjardins, MD, PhD**, **Hyungjin Myra Kim, SC**, **Eric Good, DO**, **Krit Jongnarangsin, MD**, **Hakan Oral, MD**, **Aman Chugh, MD**, **Frank Pelosi, MD**, **Fred Morady, MD**, and **Frank Bogun, MD**
University of Michigan Medical Center, Ann Arbor, MI*

Abstract

Background—Structural factors contributing to the development of post-infarction ventricular tachycardia (VT) are unclear. The purpose of this study was to analyze infarct architecture and electrogram characteristics in patients with and without inducible VT and to identify correlates of post-infarction VT.

Methods and Results—Twenty-four post-infarction patients (median age 64 [53,70] years) were referred for radiofrequency catheter ablation of VT (n=12) or frequent symptomatic premature ventricular contractions (PVCs, n=12). Delayed-enhanced magnetic resonance imaging (DE-MRI) was obtained prior to ablation. Electroanatomical mapping was performed and scar area and electrogram characteristics of the scar tissue were compared in patients with and without inducible VT.

The median ejection fraction in subjects with and without inducible VT was 27% [22,43] and 43% [40,47], respectively (p=0.085). Subendocardial infarct area determined by DE-MRI was larger in patients with inducible VT (43 [38,62] cm^2) than those who were non-inducible (8 [4,11] cm^2, p=0.002), and unipolar and bipolar voltages on electroanatomical maps were significantly lower in inducible patients (both p<0.05). An infarct volume of >14% identified 11 of 12 patients with inducible VT (AUC 0.94, p=0.007). On electroanatomical mapping, distinct sites with isolated potentials (IPs) were more prevalent in inducible than noninducible patients (13.2% vs. 1.1% of points within scar; p<0.001). The number of inducible VTs correlated with the number of distinct sites with IPs (R=0.87, p<0.0001).

Conclusions—Scar tissue in post-infarction patients with inducible VT shows quantitative and qualitative differences from scars in patients without inducible VT. Scar size and IPs are correlated with VT inducibility.

Keywords

mocardial infarction; ventricular tachycardia; isolated potentials; scar; magnetic resonance imaging

Prior studies have suggested that the severity of ventricular arrhythmias after myocardial infarction is related to the extent of myocardial injury.(1–3) However, ventricular arrhythmias do not invariably occur in patients with large infarcts.(4) It may be that survival of myocardial fibers explains why arrhythmias occur in some but not other patients.(4) The purpose of the study was to compare infarct architecture as determined by delayed enhanced

Corresponding author: Frank Bogun, MD, Cardiovascular Center, SPC 5853, 1500 East Medical Center Drive, Ann Arbor, Michigan 48109-5853, Tel. 734-936-5606, Fax 734-936-7026, fbogun@med.umich.edu.

Conflict of Interest Disclosures: Dr Bogun participated in a catheter study by Biosense Webster. None of the remaining authors have any relationships to disclose.

magnetic resonance imaging (DEMRI), infarct size, and electrogram characteristics between post-infarction patients with and without inducible ventricular tachycardia (VT).

Methods

Patient Characteristics (Table 1)

The subjects of this study were a consecutive series of 24 patients with post-infarction ventricular arrhythmias who were referred for catheter ablation with no contraindications for myocardial magnetic resonance imaging (MRI). Based on the results of the electrophysiology study, they were stratified into two groups: those in whom VT was inducible, and those in whom it was not. None of the patients had prior ablation procedures.

Magnetic Resonance Imaging

Before the electrophysiology procedure, all patients underwent DE-MRI. The studies were performed on a 1.5 Tesla magnetic resonance imaging scanner (Signa Excite CV/i, General Electric, Milwaukee, Wis.) with a 4- or 8-element phased array coil placed over the chest of patients in the supine position. Images were acquired with ECG gating during breath-holds. Dynamic short- and long-axis images of the heart were acquired using a segmented k-space, steady-state, free-precession pulse sequence (repetition time 4.2 ms, echo time 1.8 ms, 1.4×1.4 mm in-plane spatial resolution, 8 mm slice thickness). Fifteen minutes after administration of 0.20 mmol/kg of intravenous gadolinium DTPA (Magnevist, Berlex Pharmaceuticals, Wayne, NJ), 2-D delayed enhancement imaging was performed using an inversion-recovery sequence (5) (repetition time 6.7 ms, echo time 3.2 ms, in-plane spatial resolution 1.4 × 2.2 mm, slice thickness 8 mm) in the short-and long-axis of the left ventricle at matching cine-image slice locations. The inversion time (250–350 ms) was optimized to null the normal myocardium.

All DEMRI images were analyzed off-line with specialized post-processing software (Cinetool, General Electrics, Milwaukee). For each subject, manual tracing of the endocardial contour of delayed enhanced images was performed on a stack of 15–20 short axis images, from base to apex of the left and right ventricles. The area of delayed enhancement was then automatically determined by a region growing algorithm as the area encompassing pixels with values ≥ M/2, using the traditional method of Full Width Half Maximum.(6) Then the percentage of peri-infarct zone was computed analogous to prior reports (7,8) All contours were exported for further processing with customized software using Matlab (Mathworks, Natick, MA) to generate panoramic views representing the circumferential extent of delayed enhancement from base to apex of the left and right ventricles. Subendocardial infarct area and infarct burden were measured(9). The infarct percentage was defined as the proportion of scar volume divided by the total myocardial volume.

Electrophysiology Procedure

A quadripolar electrode catheter was positioned in the right ventricle. Programmed stimulation was performed at the right ventricular apex and outflow tract using up to 3 drive cycle lengths and up to four extrastimuli.(10) Isoproterenol was not used during programmed stimulation. All sustained, monomorphic VT morphologies that were induced prior to ablation were recorded and classified by 2 independent observers as identical or distinct if multiple VTs were induced. Only VT that was sustained was included. Sustained, VT was defined as lasting ≥30 seconds or requiring termination <30 seconds secondary to hemodynamic intolerance. The protocol was performed in a similar manner in both patient groups and was finished only when the entire protocol was concluded from 2 right

ventricular sites. Systemic heparinization with a target activated clotting time of approximately 300 seconds was maintained throughout the procedure.

Mapping Procedure

An electroanatomical mapping system (CARTO, Biosense Webster Inc, Diamond Bar, CA) was used in all patients. The mapping/ablation catheter was a 3.5-mm irrigated-tip catheter. A 2-mm ring electrode was separated from the distal electrode by 1 mm (Thermocool, Biosense Webster Inc, Diamond Bar, CA). Intracardiac electrograms were filtered at 50–500 Hz. The intracardiac electrograms and leads V_1, I, II and III were displayed on an oscilloscope and stored on optical discs (EP Med, West Berlin, NJ).

Left ventricular access was obtained using a retrograde aortic approach. A sinus rhythm voltage map was performed in all patients. Bipolar pace-mapping at an output of 10 mA and a pulse width of 2 ms was performed to identify VT reentry circuit exit sites and the sites of origin of PVCs. In patients with frequent PVCs, activation mapping was also performed.

Analysis of Mapping Data

Scar was defined by a voltage <1.0 mV(11). Scar size was measured with the CARTO 7.0 software (CARTO, Biosense Webster Inc, Diamond Bar, CA; Figures 1a and 2a).

Mapping sites were considered distinct if they were separated by ≥5 mm. Bipolar electrograms were classified by 2 independent observers. Differences were resolved by consensus according to the following criteria (12) that were modified and adapted to the catheter and recording system used in this study(13):

1. Normal electrograms: sharp biphasic or triphasic spikes with amplitudes ≥3 mV and duration <70 ms, and/or amplitude:duration ratio >0.046.
2. Fractionated electrograms: amplitude ≤0.5 mV, duration ≥133 ms, and/or amplitude:duration ratio <0.005.
3. Isolated potential: a potential separated from the ventricular electrogram by an isoelectric segment or a segment with low amplitude noise (<0.05mV) of >20 ms duration at a gain of 40–80 mm/mV.
4. Electrograms that did not fit the above 3 categories were defined as non-fractionated abnormal electrograms.

If a site with an isolated potential was identified, higher resolution mapping was performed to allow demarcation of an area where contiguous isolated potentials were identified. An area with isolated potentials was considered distinct if it was surrounded by sites devoid of isolated potentials (Figure 2a) (14). For hemodynamically tolerated VTs, a site was considered an isthmus site if 1 or more of the following criteria was present: 1) Concealed entrainment with VT termination during radiofrequency ablation; 2) mechanical termination of VT with the catheter located at a certain location and VT was no longer inducible after radiofrequency ablation. For non-tolerated VTs, a matching pace-map and non-inducibility of VT after ablation were the criteria for a critical isthmus. A prior study demonstrated that these criteria are present at critical isthmus sites. (13)

Radiofrequency Ablation

Radiofrequency catheter ablation was performed at the critical isthmus sites of VT or at the site of origin of PVCs. Radiofrequency energy was delivered at 30–50 watts targeting an impedance drop of 10 Ohms with a maximal temperature of 45°C. If VT or spontaneous

PVCs terminated during radiofrequency ablation, another application of radiofrequency energy was delivered at the same site.

Follow-up

Patients who received an ICD were seen every 3–6 months in the ICD clinic. Patients who underwent PVC ablation were seen 3, 12 and 24 months post ablation and had a repeat Holter 3 months post ablation.

Methodological Analysis

In order to identify the correlates of post-infarction VT, the EGM characteristics of the arrhythmogenic substrate including voltage, EGM width, and the prevalence of abnormal EGMs, fractionated EGMs, and isolated potentials within the infarct region were compared between patients with and without inducible VT. MRI findings which could identify patients at risk of post-infarct arrhythmia, such as left ventricular ejection fraction, infarct percentage, endocardial infarct area, infarct volume, percent of endocardial scar area, peri-infarct zone percentage of scar, and percantage of peri-infarct zone percentage, were also compared between the 2 groups.

Statistical Analysis

Data analysis was conducted using SAS vs 9.1 (Cary, NC). Continuous data were evaluated for normality and were then compared between those with and without VT using either Student's t or Wilcoxon rank sum testing for normal and non-normal data, respectively, with values expressed as mean± standard error or median [25^{th}, 75^{th} percentile] as appropriate. Categorical data were compared with Fisher's exact test.

Odds ratios [95% confidence interval] for non-repeated data were generated using logistic regression. For repeated measures (EGM width, unipolar and bipolar voltage), the distribution of data points was evaluated for normality then the mean or median of each repeated variable was taken for each patient as appropriate. These data were then compared across groups using independent sample t-tests or Wilcoxon rank sum testing as appropriate.

A receiver operating characteristic curve (ROC) for DE-MRI scar percentage and VT inducibility was generated and the area under the curve (AUC) was calculated. Scar percentage threshold was selected as that displaying optimal sensitivity and specificity for VT discrimination.

Mixed model linear regression for repeated measures (random intercept) was then used to compare the unipolar voltage, bipolar voltage, and EGM widths between those with VT and those without. Voltages obtained on electroanatomical mapping were dichotomized at the previously published threshold of <1mV(11), and the number of points at this threshold were compared between groups with Wilcoxon testing, and logistic odds ratios for VT inducibility were generated.

For all analyses, a $p<0.05$ was considered statistically significant. This study was approved by the University of Michigan Medical Institutional Review Board.

Results

Characteristics of the cohort are shown in Table 1. Of the 24 subjects, 12 had clinical VT and 12 had symptomatic premature ventricular complexes (PVCs). All patients had a history of myocardial infarction, predating the catheter ablation procedure by a median of 5 [1, 12] years. Three of the patients with VT were treated with amiodarone within six weeks before

the procedure. Two of the PVC patients had been treated with amiodarone within six weeks before the procedure.

Inducibility of VT

A total of 37 VTs (mean cycle length 296±58 ms) were induced in 11/24 patients. Twenty-eight VTs had a right bundle branch block morphology and 9 had a left bundle branch block morphology. The other 13 patients had no inducible, sustained, monomorphic VT. Ten with inducible VT had a clinical history of sustained VT and one patient with inducible VT had no clinical history of VT. In this patient, 4 monomorphic VTs were induced. One patient had clinical VT and PVCs, but only PVCs were inducible.

Electrogram Characteristics of Patients With and Without Inducible VT (Table 2)

In patients with inducible VT, 124±94 endocardial points (range 56–255 points) were registered during sinus rhythm, compared to 148±117 points (range 37–416 points) in patients without inducible VT (p=0.0001). The number of distinct points sampled within scar tissue in patients with inducible VT was 30 [28,43] points vs. 9 [6,19] points in noninducible patients (p=0.003). This resulted in a point density of 0.94 [0.79,1.22] points/cm^2 in patients with inducible VT compared to 1.25 [1.12,1.64] points/cm^2 in patients without inducible VT (p=0.01).

Distinct sites with isolated potentials (IPs) were found almost exclusively in patients who had inducible VT, comprising 13.2% of the endocardial electrograms sampled in the scar areas (Table 2). In patients in whom VT could not be induced, less than 1.1% of the scar electrograms displayed IPs (P<0.0001). In patients with inducible VT, 47.4% of the sites within scar displayed fractionated electrograms, compared to 26.9% of sites within scar in patients without inducible VT (p=0.0001). Sixty-four percent of the critical isthmus sites of reentrant VT displayed isolated potentials; 18% had fractionated electrograms, and another 18% showed non-fractionated abnormal electrograms.

Individuals with inducible VT had significantly lower unipolar and bipolar voltages and longer EGM widths than those without VT (Table 2). Accounting for correlated intrapatient data on repeated measures analysis, individuals with VT had a 71±18% lower unipolar voltage (p=0.011) and 10±5.0% lower bipolar voltage (p=0.004) than those without VT.

Inducible VTs and Critical Isthmus Areas

In patients with inducible VT, there was an association between the number of distinct sites with isolated potentials and the number of inducible VTs (R=0.77; p=0.005). If non-inducible patients are included in the analysis, this association is stronger (R=0.87; p<0.0001; Figure 3). Across the cohort, the odds [95% CI] of having inducible VT increased by 2.7 times [1.2,6.4] for each distinct site at which an IP was recorded during the mapping procedure (p=0.0043). Infarct size as assessed by electroanatomical mapping also correlated with the number of inducible VTs (R=0.74, p<0.0001). In every patient with inducible VT, at least one critical isthmus of the VT reentry circuit was identified.

Inducibility of VT and infarct size on DE-MRI (Table 3)

While MRI derived ejection fraction was not statistically different between groups, there was a trend toward a lower ejection fraction in those with VT (Table 1). All DE-MRI measures of infarct size (infarct volume, infarct % and endocardial infarct area) were associated with VT inducibility (Table 3). The odds of VT inducibility increased 40% (odds ratio 1.4 [1.1,1.7]) for each percentage of endocardial scar measured on DE-MRI. By ROC analysis (Figure 4), a scar burden of ≥ 14% on DE-MRI offered 100% sensitivity and 92% specificity for differentiating inducible and non-inducible patients (AUC 0.94; p=0.007).

The peri-infarct zone in inducible patients was larger than in patients without inducible VT. If however the proportion of peri-infarct zone within the scar was compared, there was no difference between inducible and non-inducible patients.

Impact of Infarct Age

Patients without inducible VT tended to have more recent infarcts than patients with inducible VT (Table 1). Among the 12 patients referred for catheter ablation of VT, there was a significant correlation between infarct age and the number of sites with isolated potentials per patient ($R=0.56$; $p<0.01$). The percentage of non-fractionated abnormal electrograms in the scar tissue was inversely related to infarct age ($R=-0.55$; $p=0.006$). The older the scar, the higher the percentage of isolated potentials within the infarct scar ($R=0.5$; $p=0.017$). The percentage of fractionated electrograms within the scar did not correlate with infarct age ($R=0.38$; $p=0.07$).

Ablation of VT and PVCs

At 14/22 isthmus sites (64%), IPs were identified during sinus rhythm; at 5 isthmus sites (23%), fractionated electrograms were present, and at the remaining 3 isthmus sites (14%), abnormal electrograms were present. Matching pace-maps were present at 19 isthmus sites, concealed entrainment was demonstrated at one isthmus site, and reproducibly inducible VT was no longer inducible with the ablation catheter at a location with a matching pace-map at 2 isthmus sites. Radiofrequency energy delivery resulted in successful ablation of all 37 VTs that were inducible before ablation. In 3 patients, post ablation, 4 VTs that were not inducible at the beginning of the procedure were induced after ablation. None of these VTs matched with pace-maps and therefore they were not targeted for ablation.

A total of 15 different PVCs were targeted in the patients with PVCs. All sites of origin of the PVCs were located within scar tissue. All were successfully ablated reducing the PVC burden from 14±13% to 0.7±1.1% on Holter monitoring.

Clinical Follow-up

All but one patient presenting with VT and all patients who had inducible VT received an implantable cardioverter-defibrillator (12/24 patients). The mean duration of follow-up was 13±12 months (range 1–43 months). Two of the patients with inducible VT received appropriate ICD therapies during follow-up. In patients with frequent PVCs, one of the patients with frequent PVCs had recurrence of frequent PVCs. These PVCs were similar in morphology to the initially targeted PVCs. None of the patients without inducible VT had documented episodes of sustained VT during follow-up.

Discussion

Main Findings

This study analyzed infarct architecture by MRI technology and electrogram characteristics in patients with and without inducible VT and identified the determinants of post-infarction VT. The results of this study demonstrate that the scars in post-infarction patients with and without inducible VT have different architectural and electrophysiological features. Infarct scars in patients with inducible VT are larger and harbor more sites with isolated and fractionated potentials. A cut-off value of 14% of scar by DE-MRI best differentiated inducible from non-inducible patients. Infarct age affects scar tissue composition and a suitable substrate for monomorphic VT may develop over time.

Infarct Structure and Determinants of Inducible VT

This is the first study of post-infarction patients with and without inducible VT in which DE-MRI and electroanatomical mapping were combined for characterization of determinants for VT inducibility. Prior studies have shown a correlation between infarct mass or tissue heterogeneity as assessed by DE-MRI and the inducibility of VT.(7,15) However, detailed information on electroanatomical mapping and electrogram characteristics in relation to MRI findings provided herein have not previously been reported.

Several studies (1–4) have pointed out that infarct size is larger in patients with post-infarction VT than in patients without post-infarction VT. This is confirmed in this study. Using receiver operator characteristics curves, a cut-off value of ≥14% for infarct percentage best separated inducible and non-inducible patients. The influence of the peri-infarct zone paralleled the impact of the scar size on inducibility. A randomized prospective study using infarct burden based on MRI as the only risk stratifier (DETERMINE), is currently under way (http://clinicaltrials.gov NCT00487279). This study will clarify the value of this parameter in patients who are candidates for ICD implantation for primary prevention of sudden cardiac death.

However, infarct mass and volume are not the only determinants of VT inducibility. The likelihood of having inducible VT was nearly 3 fold higher in the presence of an isolated potential. Also there was a significant relationship between the number of areas displaying isolated potentials and the number of inducible VTs.

Inducibility correlating with the presence of IPs was reported in a recent study by Haqqani et al (16). In contradistinction to our study, no MRIs were used and assessment of impact of infarct size and infarct architecture therefore remains speculative. Our study highlights the importance of infarct size determination by DE-MRI, which complements the assessment of electrophysiologic data and helps to begin to answer the question of arrhythmogensis. Critical areas for VT were not characterized by Haqqani et al. In our study, we demonstrated that in the majority of critical isthmus areas, IPs were present, indicating a relationship between the arrhythmogenic substrate and inducibility of VT which was further supported by the strong correlation between the number of areas with isolated potentials and the number of inducible VTs.

A prior study demonstrated that isolated potentials are a manifestation of a fixed barrier within a VT reentry circuit (17). The higher prevalence of isolated potentials in patients with inducible VT probably reflects the presence of surviving muscle bundles within scar, that serve as the substrate for slow conduction and reentrant post-infarction VTs. (18) IPs were rarely recorded in patients without inducible VT. These findings support the results of a prior study in which intraoperative mapping in patients with a history of spontaneous VT demonstrated a higher prevalence of double potentials or fractionated electrograms than in patients with frequent PVCs but no VT(19).

Electrogram Characteristics and Infarct Age

Electrogram characteristics in scar tissue have not yet been systematically compared in patients with and without inducible VT. Electrogram characteristics reflect the tissue composition within the scar(20). The predominance of non-fractionated abnormal electrograms in non-inducible patients compared to the predominance of fractionated electrograms in inducible patients indicates a higher degree of complex anisotropy, which could contribute to the genesis of sustained VT. Infarct age, probably by means of scar remodeling, impacts impulse propagation through scar tissue, potentially accounting for the higher prevalence of isolated potentials and inducible VT in patients with older infarcts.

This is supported by morphometric analysis of tissue composition in post-infarction animal models(20).

In parallel with infarct age, tissue composition (as reflected by electrogram characteristics) changes over time(20). It is possible that scar remodeling(14) influences the development of ventricular arrhythmias over time(21), which may explain the absence of isolated potentials in non-inducible patients, who also had more recent infarcts. Additional studies are necessary to clarify the temporal changes in scar architecture and electrogram characteristics after a myocardial infarction.

Limitations

The sample size in this cross-sectional study was small and the results need to be confirmed in larger studies. Longitudinal studies might help to better assess scar tissue evolution over time. A limitation of this study is that there was no control group without VT or PVC's.

Another limitation of this study was a difference in the number of sampling points between patients with and without inducible VT. Despite a larger number of sampling points in the scar of patients with inducible VT, the sampling density within the scar actually was higher in patients without inducible VT. Therefore, it is possible that IPs were under-detected in patients with inducible VT.

We performed several univariable analyses and unadjusted p values should be viewed with caution given the risk of a type I error. However, if a more stringent p value of 0.004 is used, the significance of the statistical analysis remains largely unchanged.

Clinical Implications

Cardiac MRIs may assist in risk stratification of post-infarction patients. Scar size and electrogram characteristics of patients with inducible and non-inducible VT differ significantly. Whether assessing the infarct burden based on MRI as a risk stratifier will translate in mortality benefit will be clarified by an ongoing randomized study.

References

1. Kaplinsky E, Horowitz A, Neufeld HN. Ventricular reentry and automaticity in myocardial infarction. Effect of size of injury. Chest. 1978; 74:66–71. [PubMed: 668438]
2. Roberts R, Husain A, Ambos HD, Oliver GC, Cox JR Jr, Sobel BE. Relation between infarct size and ventricular arrhythmia. Br Heart J. 1975; 37:1169–75. [PubMed: 53056]
3. Califf RM, Burks JM, Behar VS, Margolis JR, Wagner GS. Relationships among ventricular arrhythmias, coronary artery disease, and angiographic and electrocardiographic indicators of myocardial fibrosis. Circulation. 1978; 57:725–32. [PubMed: 75774]
4. Bolick DR, Hackel DB, Reimer KA, Ideker RE. Quantitative analysis of myocardial infarct structure in patients with ventricular tachycardia. Circulation. 1986; 74:1266–79. [PubMed: 3536152]
5. Simonetti OP, Kim RJ, Fieno DS, Hillenbrand HB, Wu E, Bundy JM, Finn JP, Judd RM. An improved MR imaging technique for the visualization of myocardial infarction. Radiology. 2001; 218:215–23. [PubMed: 11152805]
6. Amado LC, Gerber BL, Gupta SN, Rettmann DW, Szarf G, Schock R, Nasir K, Kraitchman DL, Lima JA. Accurate and objective infarct sizing by contrast-enhanced magnetic resonance imaging in a canine myocardial infarction model. J Am Coll Cardiol. 2004; 44:2383–9. [PubMed: 15607402]
7. Schmidt A, Azevedo CF, Cheng A, Gupta SN, Bluemke DA, Foo TK, Gerstenblith G, Weiss RG, Marban E, Tomaselli GF, Lima JA, Wu KC. Infarct tissue heterogeneity by magnetic resonance imaging identifies enhanced cardiac arrhythmia susceptibility in patients with left ventricular dysfunction. Circulation. 2007; 115:2006–14. [PubMed: 17389270]

8. Yan AT, Shayne AJ, Brown KA, Gupta SN, Chan CW, Luu TM, Di Carli MF, Reynolds HG, Stevenson WG, Kwong RY. Characterization of the peri-infarct zone by contrast-enhanced cardiac magnetic resonance imaging is a powerful predictor of post-myocardial infarction mortality. Circulation. 2006; 114:32–9. [PubMed: 16801462]
9. Desjardins B, Crawford T, Good E, Oral H, Chugh A, Pelosi F, Morady F, Bogun F. Infarct architecture and characteristics on delayed enhanced magnetic resonance imaging and electroanatomic mapping in patients with postinfarction ventricular arrhythmia. Heart Rhythm. 2009; 6:644–51. [PubMed: 19389653]
10. Hummel D, Strickberger S, Daoud E, Niebauer M, Bakr O, Man K, Williamson B, Morady F. Results and efficency of programmed ventricular stimulation with four extrastimuli compared with one, two, and three extrastimuli. Circulation. 1994; 90:2827–2823. [PubMed: 7994827]
11. Callans DJ, Ren JF, Michele J, Marchlinski FE, Dillon SM. Electroanatomic left ventricular mapping in the porcine model of healed anterior myocardial infarction. Correlation with intracardiac echocardiography and pathological analysis. Circulation. 1999; 100:1744–50. [PubMed: 10525495]
12. Josephson, M. Clinical Cardiac Electrophysiology Techniques and Interpretations. Lea & Febiger; 1993.
13. Bogun F, Good E, Reich S, Elmouchi D, Igic P, Lemola K, Tschopp D, Oral H, Chugh A, Pelosi F, Morady F. Isolated Potentials During Sinus Rhythm and Pace-Mapping Within Scars as Guides for Ablation of Post-Infarction Ventricular Tachycardia. J Am Coll Cardiol. 2006; 47:2013–2019. [PubMed: 16697318]
14. Bogun F, Krishnan S, Siddiqui M, Good E, Marine JE, Schuger C, Oral H, Chugh A, Pelosi F, Morady F. Electrogram characteristics in postinfarction ventricular tachycardia: effect of infarct age. J Am Coll Cardiol. 2005; 46:667–74. [PubMed: 16098433]
15. Bello D, Fieno DS, Kim RJ, Pereles FS, Passman R, Song G, Kadish AH, Goldberger JJ. Infarct morphology identifies patients with substrate for sustained ventricular tachycardia. J Am Coll Cardiol. 2005; 45:1104–8. [PubMed: 15808771]
16. Haqqani HM, Kalman JM, Roberts-Thomson KC, Balasubramaniam RN, Rosso R, Snowdon RL, Sparks PB, Vohra JK, Morton JB. Fundamental Differences in Electrophysiologic and Electroanatomic Substrate Between Ischemic Cardiomyopathy Patients With and Without Clinical Ventricular Tachycardia. J Am Coll Cardiol. 2009; 54:166–173. [PubMed: 19573735]
17. Bogun F, Bahu M, Knight B, Weiss R, Goyal R, Daoud E, Man K, Strickberger S, Morady F. Response to pacing at sites of isolated diastolic potentials during ventricular tachycardia in patients with previous myocardial infarction. J Am Coll Cardiol. 1997; 30:505–13. [PubMed: 9247525]
18. de Bakker JM, van Capelle FJ, Janse MJ, Tasseron S, Vermeulen JT, de Jonge N, Lahpor JR. Slow conduction in the infarcted human heart. 'Zigzag' course of activation. Circulation. 1993; 88:915–26. [PubMed: 8353918]
19. Klein H, Karp RB, Kouchoukos NT, Zorn GL Jr, James TN, Waldo AL. Intraoperative electrophysiologic mapping of the ventricles during sinus rhythm in patients with a previous myocardial infarction. Identification of the electrophysiologic substrate of ventricular arrhythmias. Circulation. 1982; 66:847–53. [PubMed: 7116600]
20. Gardner PI, Ursell PC, Fenoglio JJ Jr, Wit AL. Electrophysiologic and anatomic basis for fractionated electrograms recorded from healed myocardial infarcts. Circulation. 1985; 72:596–611. [PubMed: 4017211]
21. Wilber DJ, Zareba W, Hall WJ, Brown MW, Lin AC, Andrews ML, Burke M, Moss AJ. Time dependence of mortality risk and defibrillator benefit after myocardial infarction. Circulation. 2004; 109:1082–4. [PubMed: 14993128]

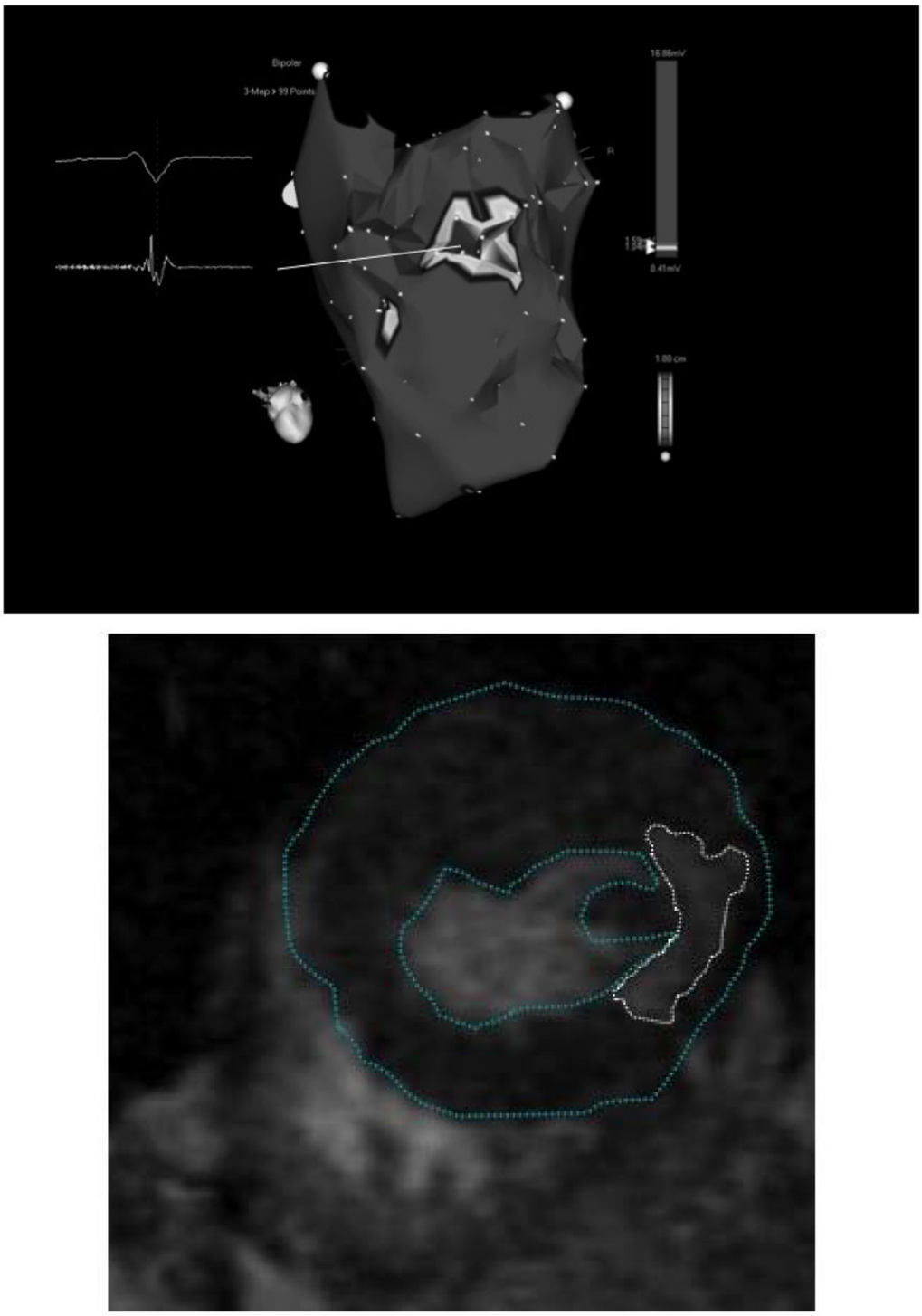

Figure 1.

Figure 1 a - Voltage map of the posterior left ventricle in a patient with prior inferior wall infarction without inducible VT. There is a localized area of low voltage that corresponds to the area of delayed enhancement in Figure 1b. The endocardial low voltage area was 4.8 cm^2 as measured by electroanatomical mapping. This patient did not display any isolated potentials during sinus rhythm. The insert shows a non-fractionated abnormal electrogram

within the scar tissue. Mitral valve annulus (MVA) and left ventricular apex (apex) are indicated.

Figure 1b - Short-axis delayed enhanced magnetic resonance image of the mid left ventricle in the same patient shown in Figure 1a. There is delayed enhancement in the posteroseptal left ventricle (encircled with dotted line). The endocardial and epicardial borders were manually traced (blue colored lines). Infarct volume was 7.6 cm^3 and the infarct percentage was 9%.

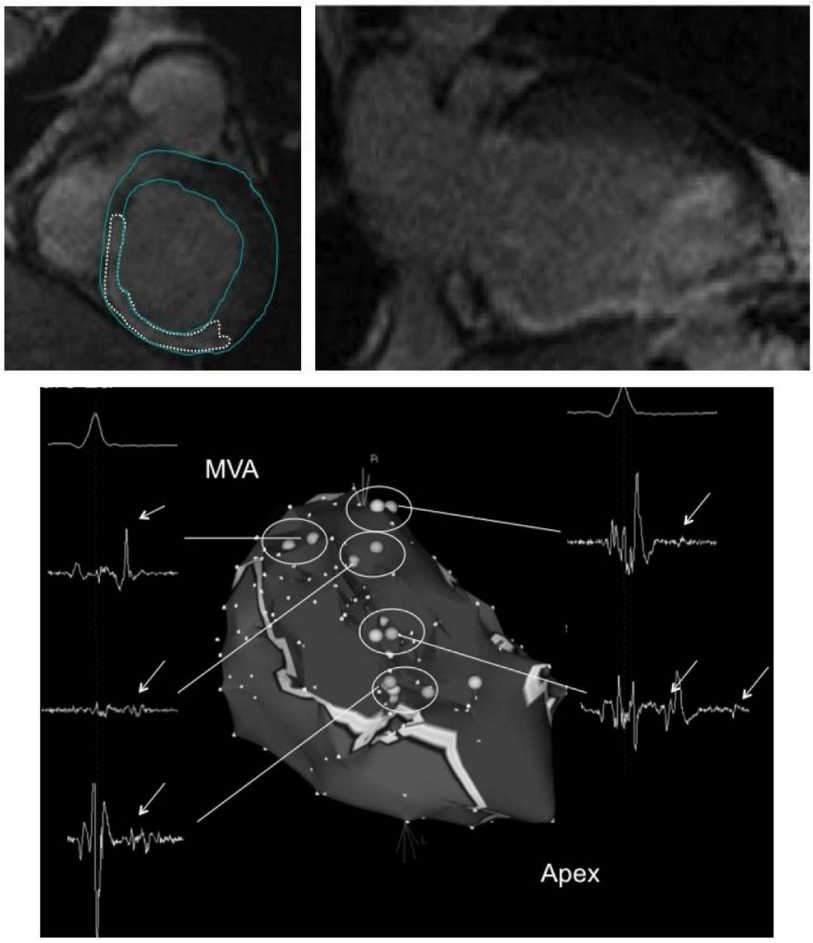

Figure 2.

Figure 2a - Voltage map of the posteroseptal aspect of the left ventricle in a patient with extensive inferoseptal wall infarction in whom 8 different VTs were induced. Areas in red indicate subendocardial scar (voltage <1.0mV). Scar area as assessed by electroanatomic mapping was 57 cm^2. Light blue tags indicate sites of isolated potentials. The inserts display the local electrograms at these sites. Isolated potentials are indicated with white arrows. There were 5 distinct sites where isolated potentials were identified (circles). Different critical VT isthmuses were identified at 3/5 sites displaying an isolated potential. The pink tags indicate isthmus sites that were identified during the ablation procedure. The mitral valve annulus (MVA) and left ventricular apex (apex) are indicated.

Figure 2b - Left panel: Short-axis delayed enhanced magnetic resonance image of the left ventricle in the same patient shown in Figure 2a. There is delayed enhancement in the inferoseptal left ventricular wall (encircled with a dotted line). Epicardial and endocardial borders are traced with a blue line. Right panel: Long-axis view of the delayed enhanced magnetic resonance image in the same patient. This shows that the scar extends from the mitral valve annulus to the left ventricular apex. The infarct volume was 27.2 cm^3 and the infarct percentage was 27%.

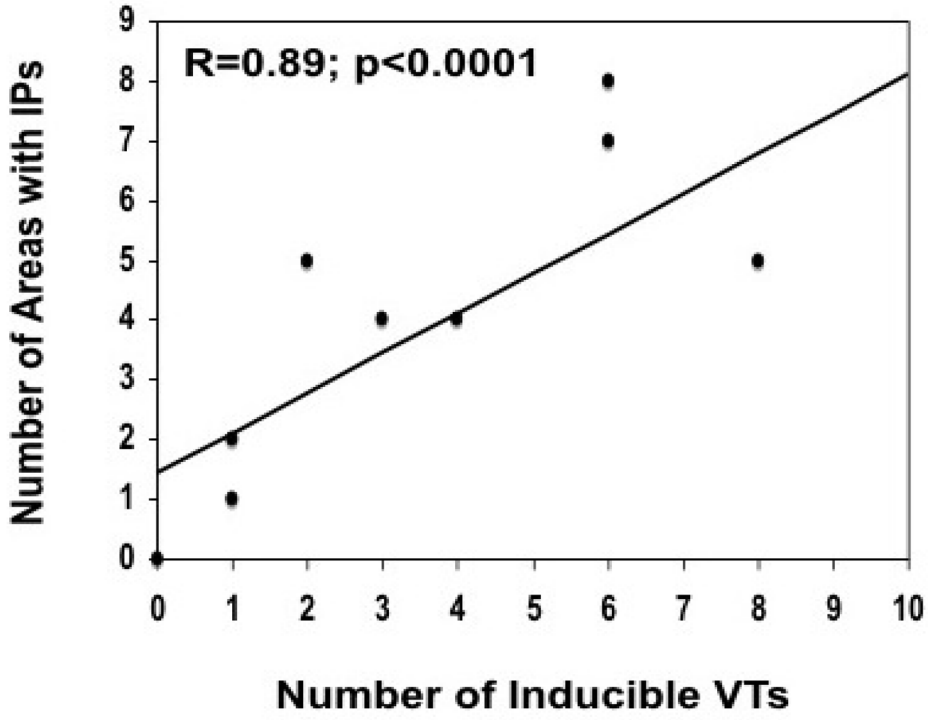

Figure 3.
Correlation between number of inducible VTs and the number of distinct sites displaying an isolated potential (IP).

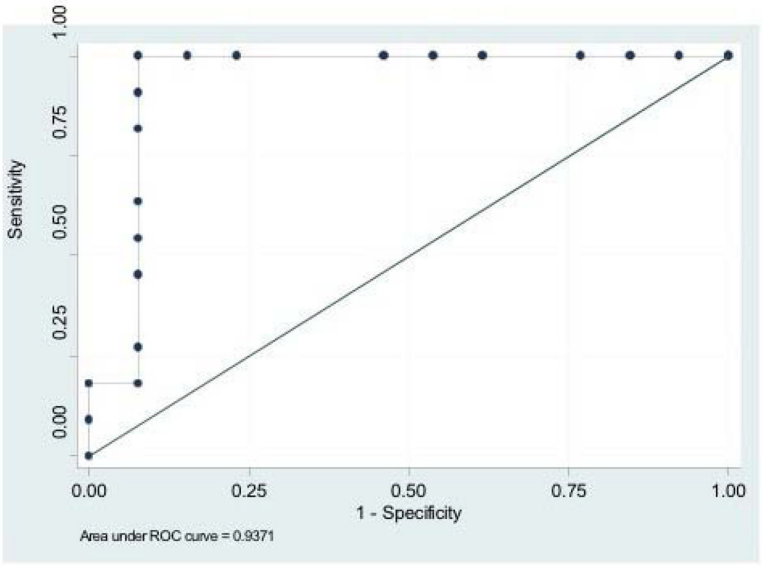

Figure 4.
Receiver operator characteristics curve indicating sensitivity and specificity for VT inducibility based on the percentage of scar by DE-MRI.

Table 1

Patients Characteristics

	Inducible VT	Non-inducibleVT	p-value
Patients, n	11	13	
Number of inducible VT per patient	3 [1,6]*	0 [0,0]*	0.0002
Patients age, years	65 [59,72]*	58 [49,69]*	0.25
Infarct age, years	12 [1,16]*	3.5 [1.5,8.5]*	0.20
Women/men, n	3/8	2/11	0.63
Ejection fraction (MRI), %	27 [22,43]*	43 [40,47]*	0.09
Infarct location, n			
Inferior	8	4	0.30
Inferolateral	2	5	0.67
Anterior	3	3	1.00
Anterolateral	0	1	1.00
Amiodarone Use, n	3	2	0.63

*Median [25th, 75th percentile]

Abbreviations: VT= ventricular tachycardia; PVC= premature ventricular complexes; MRI= magnetic resonance imaging

Table 2

Electrogram Characteristics of Scar Tissue in Patients Presenting with and without inducible VT

	Inducible VT (N=1672)	Non-Inducible (N=2460)	P value
Number of distinct points sampled	30 [28,42]	9 [6,19]	0.003
Number of distinct points sampled per 1 cm^2 infarct area	0.94 [0.79,1.22]	1.25 [1.12,1.64]	0.01
Unipolar EGM Voltage (mV)	3.2 [2.7,3.8]	6.1 [4.9,9.8]	<0.001
Bipolar EGM Voltage (mV)	0.46±0.28†	0.58±0.25†	<0.001
Area of bipolar voltage <1.0mV (cm^2)	32 [27,57]	7.4 [4.8,15]	0.003
EGM width (msec)	107[100,120]	89[85,97]	0.007
Normal EGM (%)	0	0	NS
Abnormal EGM (%)	39.2	71.8	<0.001
Fractionated EGM (%)	47.4	26.9	<0.001
EGM with Isolated Potentials (%)	13.2	1.1	<0.001

†mean ± standard deviation. All other continuous data presented as median [25, 75 percentile].

Abbreviations: EGM= electrograms

Table 3

Comparison of Infarct Size and Architecture on DE-MRI

	Inducible VT (N=11)	Non-Inducible (N=13)	p-value¶
Ejection fraction (MRI), %	27 [22,43]*	43 [40,47]*	0.09
Infarct % DE-MRI	35 [28,49]*	9 [7,12]*	0.002
Endocardial Infarct Area (cm^2) DE- MRI	43 [38,62]*	8 [4,11]*	0.002
Infarct volume (cm^3)	36 [26,42]*	5.6 [3.6,8.0]*	0.002
Endocardial scar area DE-MRI (%)	19 [15,22]*	4.9 [3.0,5.0]*	0.002
Peri-infarct zone % of scar	43 [34,52]*	40[36,56]*	0.38
Peri-infarct zone % of myocardial volume	6.2 [4.8,7.1]*	2.6[2.15.6]*	0.01

¶obtained by Wilcoxon rank sum. DE-MRI= delayed enhanced magnetic resonance imaging,

*median [25^{th}, 75^{th} percentile].